
N. Ikegaya

Characteristics of scalar dispersion from a continuous area source over a cubical array

Naoki Ikegaya[1], Aya Hagishima[2] and Jun Tanimoto[2]

[1] *IGSES, Kyushu University, Kasugakouen6-1, Kasuga-shi, Fukuoka, Japan, ikegaya@cm.kyushu-u.ac.jp*
[2] IGSES, Kyushu University, Kasugakouen6-1, Kasuga-shi, Fukuoka, Japan

1. Introduction

Understanding transport mechanisms for momentum or scalar between urban surfaces and the atmosphere is one of essential issues so as to predict flow and scalar distributions attributed to complicated urban climates. One of methods to relate these vertical distributions and surface effects such as momentum sink or scalar source/sink, is known as a similarity theory within the inertial sub-layer. In the case of the neutral stratification, especially, various investigations have revealed surface geometric dependency of aerodynamic parameters such as the drag coefficient, roughness length and displacement height by means of both field measurements and wind-tunnel experiments (For example, Cheng & Castro 2002, Hagishima et al. 2009). Moreover, similarity of the parameters between scalar and momentum has been also confirmed to be possibly applicable for urban surfaces (Kanda and Moriizumi, 2009).

In addition to the similarity theory in the inertial sub-layer, several features of flow distribution and turbulent statistics have been studied in the roughness sub-layer and canopy layer where the flow is directly affected by the existence of roughness elements. For instance, it is known that spatial-averaged velocity profile satisfies logarithmic law, even though the layer does not satisfy the premise of the similarity theory in the inertial sub-layer (Cheng & Castro, 2002). In addition, it is also revealed that characteristics of momentum transfer exists; sweep events, or strong downward motions with high momentum fluid, are dominant near roughness elements whereas ejection events, or strong upward motions with low momentum fluid, dominate sweep events in upper part of the roughness sub-layer (Raupach, 1981). Moreover, the visualization of turbulent structures around these events based on numerical simulations shows the existences of hair-pin and head-down hair-pin like vortices (For example, Finnigan et al. 2009).

In contrast to these extensive understanding of characteristics of flow fields, little of features for scalar dispersion are known especially within the roughness sub-layer. Although a few studies have revealed that there is similarity between scalar and momentum transport to some extent also in the roughness sub-layer (Boppana et al. 2013), holistic understanding of scalar transport in the layer and the canopy layer has not been reached yet.

Therefore, we have performed a large-eddy simulation on scalar dispersion from continuous area surface located on the floor of a rough surface. As the roughness condition, a cubical array in staggered layout is selected in order to generate both of the roughness sub-layer and the canopy layer. The scalar boundary layer can develop to streamwise direction. The purposes of this study are summarized as follows: (1) to quantify the streamwise characteristics of scalar boundary layer, including trends of concentration and turbulent scalar flux, (2) to apply quadrant analysis so as to quantify the contribution of updraft or downdraft to total turbulent scalar flux, and then to discuss the similarity and dissimilarity of momentum and scalar in terms of flux decomposition.

2. Numerical setups

A simulation model called parallelized large-eddy simulation model (PALM, Letzel et al. 2008) is adopted in this study. The model employs the filtered Navier-Stokes (NS) equations, the continuity equation, the equation for scalar conservation, and the equation of the sub-grid scale turbulence kinetic energy (SGS-TKE) with a turbulence model of the 1 1/2th order Deardorff scheme (Deardorff, 1980). Numerical schemes are the 3rd order Runge-Kutta scheme for time integration and the 2nd order central difference scheme for advection. The pressure and velocity are corrected by applying the fractional step method. Further details of the simulation model can be referred in Letzel et al.(2008).

The schematic figure of the simulation domain is shown in Fig. 1. The wind velocity is defined as u_i (i=1,2 and 3 for u, v and w) for x_i (i=1,2 and 3 for x:streamwise, y:spanwise and z:vertical) direction. The scalar concentration is expressed as s kg/m^3. On the floor of the domain, cubes with a height of $H = 24$ mm are arranged in staggered pattern with the packing density of 7.1%. The geometrical configuration is chosen as the form drag contributes dominantly to the total drag force at the condition of the packing density based on wind-tunnel experimental data (Zaki et al., 2012). In addition, an area scalar source are installed on the floor of the domain with the streamwise distance of $45H$.

On the wall surface, the wall function of zo-type log-law ($z_o = 3 \times 10^{-6}$ m for momentum and scalar) is employed and the surface scalar concentration is fixed as $s_{surf} = 0.17$ kgm^{-3}. The selection of the wall function and the parameter may not affect largely flow fields because the pressure form drag acting on cubical blocks is the dominant momentum sink. Although the amount of scalar fluxes on the area source is only determined by the wall

function and the parameter, it can be assumed that the scalar concentration filed is well captured after emitted from the source because the scalar is passively transported by following the flow fields.

For the lateral and streamwise boundary, the periodic boundary condition is applied and the flow is driven by the streamwise constant pressure gradient with the friction velocity of $u^* = 0.2$ after Hagishima et al. (2009) to obtain approximately 2 m/s[1] at $z = 6H$. In order to simulate a developing scalar concentration fields by a continuous area source, the concentration are reduce to its reference level $s_{ref} = 0.009$ kg/m^3 at the upstream edge of the simulation domain. For the top of the domain, the zero-gradient condition is imposed. The uniform grid size of $\Delta x_i = H/16$ are used for all directions.

The initial duration is from time $t = 0$ to 50s, which satisfies the criteria for the initial duration of 200T ($T = H/u^*$) suggested in Coceal et al. (2006) and the convergence of the temporally-spatially averaged profiles are confirmed for the streamwise wind speed, the vertical momentum flux, and turbulence kinetic energy. The averaged scalar concentration is recorded in each unit consisting of a block and a unit area from unit 1 to unit 12. Instantaneous flow and scalar fields are also collected on a xz-plane at the lateral center of blocks as shown in Fig.1.

3. Results

3.1 Validation

In Fig. 2, the transfer coefficients for momentum and scalar are compared between the simulation and experiments (Hagishima et al. 2009, Ikegaya et al. 2013) at each reference height. The transfer coefficients are defined as follows.

$$C_E = \frac{u^* s^*}{u_{ref}(s_{surf} - s_{ref})} \quad (1)$$

$$C_d = \frac{u*^2}{0.5 u_{ref}^2} \quad (2)$$

Here, u^* [m/s] is the friction velocity, $s^* = F/u^*$ [kg/m^3] is the friction scalar, F [kg/m^{2}s] is the scalar flux, and u_{ref} is the reference wind speed. As can be seen in Fig.3, it is clear that scalar transfer coefficients of the simulation are significantly underestimated, whereas the difference of the momentum transfer coefficients between the simulation and the experiments are relatively small. The ratios of the scalar transfer coefficients of the simulation to those of experiments are around 20% for all heights. This result means that the scalar flux from the surface are strongly affected by the assumption of the wall function, and it is necessary to adopt an appropriate roughness parameter to accurately reproduce the value of surface flux if we employ a wall function. In contrast to this large discrepancy of scalar transfer coefficients, the ratios of the momentum transfer coefficients between the simulation and experiments are from 88% to 99%. This is because the dominant momentum sink is attributed to the pressure form drag as we expected. In addition to the good agreement of the transfer coefficients, it is confirmed that other statistics such as the streamwise wind profile and the momentum flux are consistent with the previous experimental work (not shown here).

Fig.2 shows scalar concentrations averaged over unit 2, 3, 4, 5 and 7 for the simulation and wind-tunnel experiments (Ikegaya et al. 2012). The experimental data are measured at four points in each unit. In Fig.2 (a), the concentrations are normalized by the difference of the concentrations between the surface and the reference point. As shown in Fig.2 (a), the profiles show significantly large discrepancies between the simulation and experiment for all units. This difference seems to be caused by the underestimation of the surface flux. In addition to that, it is probable that the normalization based on the difference of the surface and reference concentrations is not

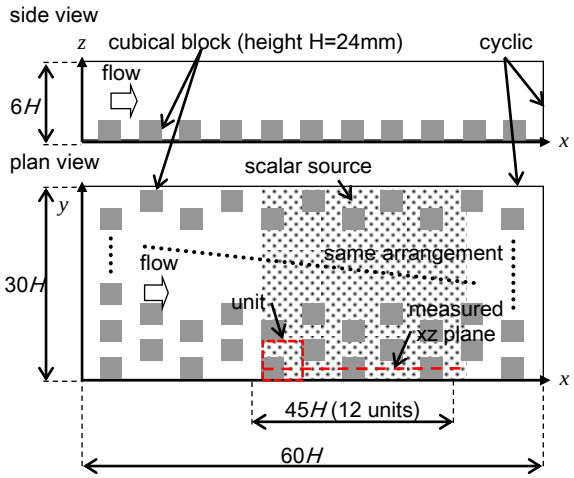

Fig. 1 Schematic view of simulation domain

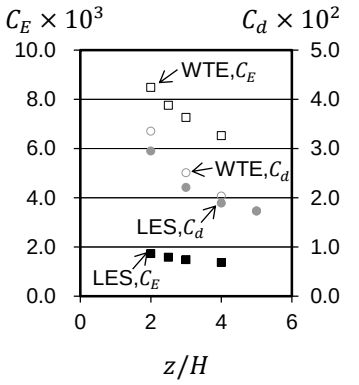

Fig. 2 Transfer coefficients

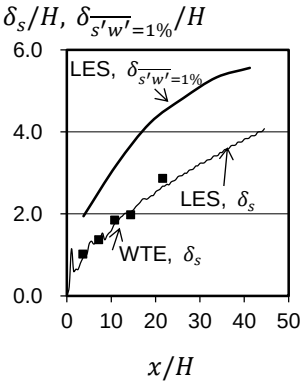

Fig. 3 Scalar boundary layer height

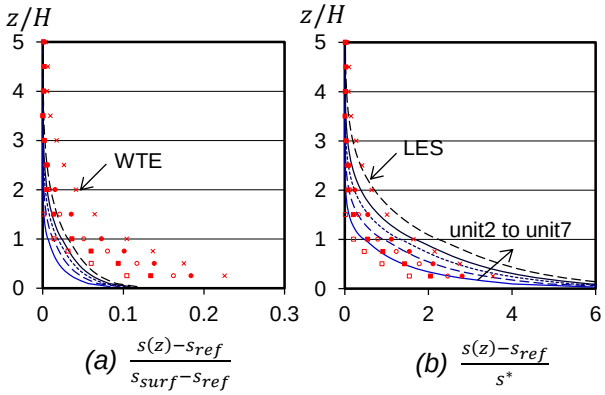

Fig. 4 Normalized scalar concentration profile over unit 2: □, unit3: ■, unit4: ○, unit5: ● and unit 7: × obtained from wind-tunnel experiments (WTE) and LES.

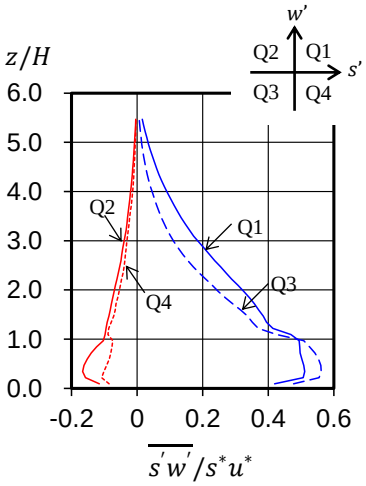

Fig. 5 Scalar turbulent flux in each quadrant

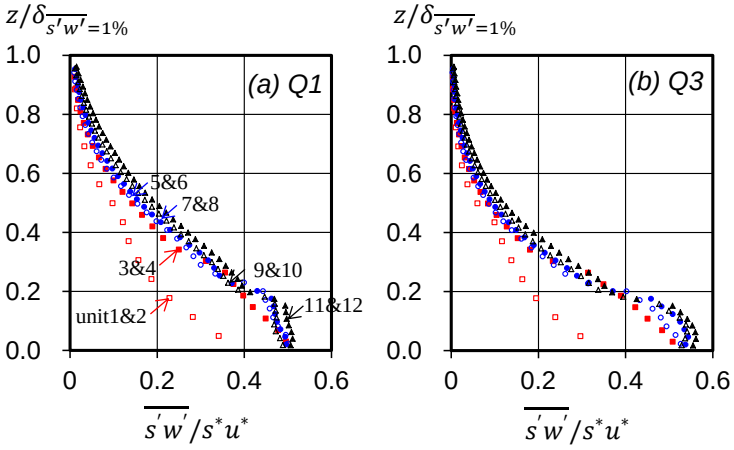

Fig. 6 Scalar turbulent flux in (a) quadrant 1 and (b) quadrant 3

appropriate for the current simulation because the concentration difference is not a potential for scalar emission from the source due to employing the wall function. According to the fact, however, that the scalar quantities are passively transported by the flow fields, the normalized concentration by considering the amount of surface flux might be suitable for the comparison with the experimental data. Therefore, in Fig.2 (b), the concentration profiles normalized by the value of friction scalar $s^* = \langle \overline{F} \rangle / u^*$ are shown, where $\langle \overline{F} \rangle$ temporally and spatially averaged surface scalar flux. The normalized values show better agreement especially above $z/H = 1$ although there are still discrepancies of the concentrations within the canopy layer. Even though the difference of the surface scalar flux is taken into accounts by the area-averaged value, streamwise changes of surface scalar flux which may not be accurately predicted will affect strongly the concentration fields above the source when continuous area source is employed. Therefore, it might be one reason of the difference for scalar concentrations in the canopy layer near the scalar source.

Based on the normalized concentrations in Fig.4 (b), 1% boundary layer thickness δ_s is calculated as shown in Fig.3 in order to compare the height obtained from the experiments (Ikegaya et al. 2012). As can be seen in Fig.3, the boundary layer heights of the simulation agree well with those of the experiments. In addition to that, the height where the scalar flux became 1% of its surface value are shown as $\delta_{\overline{s'w'}=1\%}$. This indicates that the scalar emitted from the surface reaches almost $5.6H$ with a streamwise distance of the scalar source of $45H$.

According to the comparisons of scalar fluxes and concentration fields, we can conclude that flow and scalar fields are well simulated with appropriate normalization although estimations of the surface flux by using the wall function should be improved if accurate amount of the scalar transport is necessary.

3.2 Quadrant analysis

Turbulent events of scalar transports are decomposed based on the quadrant analysis in which the intermittent events of flow and scalar are categorized by the sign of the wind speed and concentration as follows.

$$\begin{aligned} Q1&: w' > 0, s' > 0 \\ Q2&: w' > 0, s' < 0 \\ Q3&: w' < 0, s' < 0 \\ Q4&: w' < 0, s' > 0 \end{aligned} \quad (3)$$

Here, fluctuation parts of the vertical wind speed and the scalar concentration are defined as $w' = w - \overline{w}$ and $s' = s - \overline{s}$, where $\overline{w}$ and $\overline{s}$ are temporarily-averaged quantities. In the simulation, since the scalar source is located on the floor of the domain, the net scalar transfer is upward direction and events in Q1, upward drafts with high concentrations, and Q3, downward drafts with low concentrations, are expected to contribute dominantly to total scalar fluxes.

Fig. 5 illustrates the contributions of scalar fluxes in each quadrant to total surface scalar fluxes s^*u^* averaged in unit 11 and 12 up to the height $\delta_{\overline{s'w'}=1\%} \sim 5.6H$. As we expected, events in Q1 and Q3 dominate other two events in Q2 and Q4. Moreover, the contribution of Q3 is larger than that of Q1 within the canopy layer; however, opposite trends can be seen above z/H=1. For momentum transports, it is known that dominant quadrants to total momentum flux are sweep or Q4 ($u' > 0, w' < 0$) within the canopy layer, and ejection or Q2 ($u' < 0, w' > 0$) above the canopy. Since net transport directions of momentum and scalar are opposite, scalar transfer in Q3 event is related with sweep motions, and that in Q1 corresponds to ejection events. Therefore, these results mean that characteristics of the scalar and momentum transports shows similar tendency within and above canopy, indicating that the scalar quantities are transferred passively following flow fields.

In order to compare the streamwise difference of the scalar fluxes, the profiles averaged in two units are shown for events in Q1 (Fig.6 (a)) and Q3 (Fig.6 (b)). The vertical axis is normalized by $\delta_{\overline{s'w'}=1\%}(x)$ averaged over corresponding two units. The profiles show good agreement each other for both Q1 and Q3 except for the value for unit 1 and 2. The significant difference of the profile for unit1 and 2 from other downstream locations is caused by the thin boundary layer height of $\delta_{\overline{s'w'}=1\%} \sim 2H$. On the other hands, the good agreement of the profiles in other units indicates that the turbulent transport of scalar can be well explained based on the boundary layer height.

4. Conclusion

We have performed large-eddy simulation over a cubical block array with a continuous area scalar source from the floor. The characteristics of the scalar concentration fields and turbulent statistics under developing a boundary layer are revealed as follows. Firstly, normalized scalar concentration based on friction scalar shows better agreement although the surface scalar flux is not accurately estimated. The height where scalar can be transported reaches up to 5.6H with a streamwise distance of 45*H*. Secondly, quadrant analysis is performed to categorize turbulent events which contribute dominantly to scalar transfer. The analysis shows that characteristics of the scalar and momentum transports are consistent with each other within and above canopy, indicating that the scalar quantities are possibly transferred passively following flow fields.

Acknowledgment

This research was financially supported by JSPS KAKENHI Grant Number 25289196, 15K14078. The computation was mainly performed using the computer facilities at Research Institute for Information Technology, Kyushu University.

References

Boppana V.B.L., Xie Z.T., Castro I.P., 2014: Thermal stratification effects on flow over a generic urban canopy. *Boundary-Layer Meteorology*, **153**, 141-162

Cheng H., Castro I.P., 2002: Near wall flow over urban-like roughness. *Boundary-Layer Meteorology*, **104**, 229-259

Coceal O., Thomas T.G., Castro I.P., Belcher S.E., 2006: Mean flow and turbulence statistics over groups of urban-like cubical obstacles. *Boundary-Layer Meteorology*, **121**, 491-519

Deardorff J.W., 1980: Stratocumulus-capped mixed layers derived from a three-dimensional model. *Boundary-Layer Meteorology*, **18**, 495-527

Finnigan J.J., Shaw R.H., Patton E.G., 2009: Turbulence structure above a vegetation canopy. *Fluid Mechanics,* **637**, 387-424

Ikegaya N., Hagishima A., Tanimoto J., Tanaka Y., Narita K., Zaki S.A, 2012: Geometric dependence of the scalar transfer efficiency over rough surfaces. Boundary-Layer Meteorology, **143**, 357-377

Ikegaya N., Hagishima A., Tanimoto J., Tanaka Y., 2012: A study on the similarity of the momentum and scalar roughness lengths over urban-like roughness. *Transactions of Architectural institute of Japan*, **77**, 917-923 [in Japanese]

Kanda M., Moriizumi T., 2009: Momentum and heat transfer over urban-like surfaces. *Boundary-Layer Meteorology*, **131**, 385-401

Raupach M.R., 1981: Conditional statistics of Reynolds stress in rough-wall and smooth-wall turbulent boundary layers. *Fluid Mechanics*, **108**, 363-382

Letzel M.O., Karane M., Raasch S., 2008: High resolution urban large-eddy simulation studies from street canyon to neighbourhood scale. *Atmospheric Environment*, **42**, 8770-8784

Hagishima A., Tanimoto J., Nagayama K., Meno S., 2009: Aerodynamic parameters of regular arrays of rectangular blocks with various geometries. *Boundary-Layer Meteorology*, **132**, 315-337.

Zaki S.A., Hagishima A., Tanimoto J., 2012: Experimental study of wind-induced ventilation in urban building of cube arrays with various layouts. *Wind Eng. Ind. Aerodyn.*, **103**, 31-40